

Method to Improve the Linearity of Active Commutating Mixers Using Dynamic Current Injection

Mohammad-Mahdi Mohsenpour, *Member, IEEE*, and Carlos E. Saavedra, *Senior Member, IEEE*

Abstract—Dynamic and static current injection methods to improve the linearity of a current commutating mixer are investigated and a double-balanced CMOS mixer (DBM) providing high linearity is presented in this paper. A cross-coupled pair is used in the IF stage of the mixer to dynamically inject current into the mixer to provide a high linearity. The proposed DBM was fabricated using a standard 130-nm CMOS process and was tested on-wafer. The double-balanced mixer delivers 10-dB conversion gain, 9.5-dBm third-order intercept point, and input P_{1dB} of -2.4 dBm. RF bandwidth of the proposed mixer is 6 GHz, covering 0.5–6.5 GHz with an IF bandwidth of 300 MHz. RF to IF and LO to IF isolation are also better than 59 dB in the whole frequency band. The circuit uses an area of 0.015 mm² excluding bonding pads and draws 4.5 mW from a 1.2 V supply.

Index Terms—CMOS active mixer, cross-coupled current injection, current commutating mixer, dynamic current injection, high linearity, RF integrated circuits.

I. INTRODUCTION

IN SUBMICROMETER CMOS nodes with reduced power consumption, it is challenging to design active mixers with acceptable linearity, conversion gain, and noise figure (NF). Different methods have been used to overcome the tradeoff between conversion gain, NF, power consumption, and linearity measures [P_{1dB} and third-order intercept point (IIP3)] of the mixer, improving the linearity while the other metrics do not change drastically.

Harmonic distortion cancelation methods are one of the main approaches to improve linearity. In feed-forward techniques, such as the derivative superposition method [1], the third-order intermodulation product of the mixer is canceled through the use of two intermodulation terms with equal amplitude and opposite phase. Noise contribution of the additional circuitry and the dependence of the linearity improvement to the accuracy and the variation of the required phase shift are the common challenges with this technique. Injecting the intermodulation products to the mixer [2] is another

method which improves the overall performance of the mixer while, in return, the mixer consumes more power and becomes larger due to the use of inductors.

The other approach aims to reduce the severity of the above-mentioned tradeoff. This is usually implemented by providing independent bias currents for the transconductance and the switching stages [3], current bleeding [4], [5], injecting current into mixer and reducing the current in switching devices and loads [6]–[8], or current reuse and folded-switching [9]–[12] which take the advantage of pMOS–nMOS pairs to improve gain and linearity both in transconductance and IF stages. However, degraded gain performance in high frequencies, higher power consumption, and occupying larger area, are among the common designs' drawbacks.

In this paper, a novel dynamic current injection method is proposed to improve the linearity and conversion gain of the mixer. Unlike other current injection methods, in the proposed mixer, the current injection is confined to the IF stage to avoid the use of inductor and increase in the power consumption. A cross-coupled pMOS pair, derived with the LO signal, is used to dynamically inject current into the mixer, avoiding gain compression in the output nodes. This paper is an extended version of [13]. Here, static and dynamic current injection methods are studied further. Also, the design procedure of the proposed dynamically current injected mixer is provided.

II. CURRENT INJECTION CONCEPT

The IIP3 in an active commutating mixer is mostly determined by the overdrive voltage of the transconductance stage. Increasing the overdrive voltage of this stage, to achieve a better mixer linearity, leads to lower voltage headroom in the IF stage and consequently lower conversion gain. Higher load resistors and active loads [11] could be used to provide higher conversion gain, but both methods lead to linearity degradation due to the signal compression at the mixer's output. Use of external current sources in IF stage, as shown in Fig. 1, to provide part of the commutating current lets the designer improve the linearity further.

The static and dynamic current injection methods have been investigated and used widely [6]–[8] to inject current into the node P, improving linearity and flicker NF, respectively, while maintaining high conversion gain. However, the capacitive loading of the node P degrades conversion gain and consequently the NF of the mixer at high frequencies. In the method

Manuscript received June 28, 2016; revised September 22, 2016; accepted October 24, 2016. Date of publication November 18, 2016; date of current version December 7, 2016. This work was supported by the Natural Science and Engineering Research Council of Canada. An earlier version of this paper was presented at the 2016 IEEE MTT-S International Microwave Symposium, San Francisco, CA, USA, May 22–27, 2016.

The authors are with the Department of Electrical and Computer Engineering, Queen's University, Kingston, ON K7L 3N6, Canada (e-mail: m.mohsenpour@queensu.ca; saavedra@queensu.ca).

Color versions of one or more of the figures in this paper are available online at <http://ieeexplore.ieee.org>.

Digital Object Identifier 10.1109/TMTT.2016.2623698

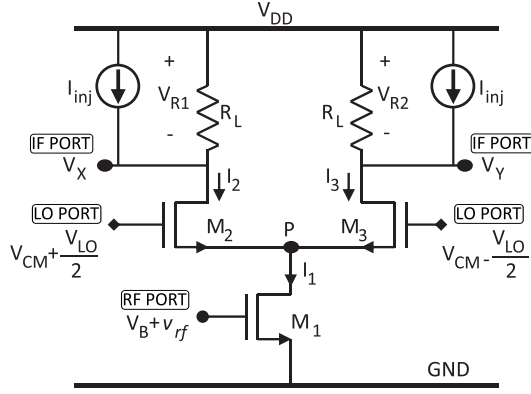


Fig. 1. Schematic of the SBM with external current injection sources.

proposed here, the current injection is implemented at the IF stage of the mixer to ensure minimum capacitive loading of the mixer at the node P.

The design process of the proposed mixer is based on improving the signal compression at the output while improving the conversion gain. Current injection leads to conversion gain, noise, and linearity metrics that could not be achieved together in conventional current commutating mixer.

In a basic single-balanced mixer (SBM) and the absence of the injected current, $I_{inj} = 0$, in Fig. 1, the output nodes voltages, V_X and V_Y , need to remain high enough to maintain M_1 in saturation and avoid M_2 and M_3 entering into the triode region when they are both turned ON and carrying current. The amplitude of the LO signal that places either M_2 or M_3 , as a differential pair, at the edge of conduction is $\sqrt{2} V_{ov2,3}$. $V_{ov2,3}$ is the overdrive voltages of M_2 and M_3 when $V_{LO} = 0$. Therefore, the minimum voltage of the output nodes, $V_{X,Y,min}$, is

$$V_{X,Y,min} = V_{ov1} + \left(1 + \frac{\sqrt{2}}{2}\right) V_{ov2,3} \quad (1)$$

where V_{ov1} is the overdrive voltages of the transconductor stage. In Fig. 1, the transconductance stage is biased by V_B while v_{rf} denotes the input RF signal. The bias voltage and the LO signal of the switching stage are indicated by V_{CM} and V_{LO} , respectively. The maximum voltage drop across load resistors, $V_{R,max}$, maximum load resistance, R_{L0} , and maximum voltage conversion gain, CG_0 , of the mixer are given by

$$V_{R,max} = \text{Max}(V_{R1,2}) = V_{DD} - V_{X,Y,min} \quad (2)$$

$$R_{L0} = R_L|_{I_{inj}=0} = \frac{V_{R,max}}{I_1} \quad (3)$$

$$CG_0 = \frac{2}{\pi} \frac{V_{R,max}}{V_{ov1}}. \quad (4)$$

Based on (1) and (2), smaller V_{ov1} and $V_{ov2,3}$ should be used to improve the voltage conversion gain of the mixer determined by (4). However, smaller V_{ov1} degrades IIP3. Therefore, the mixer's current and overdrive voltages give little room for improving gain and linearity simultaneously. Increasing R_L beyond R_{L0} in (3) results in pushing V_X and V_Y lower than $V_{X,Y,min}$. Therefore, either M_2 or M_3 enters triode region

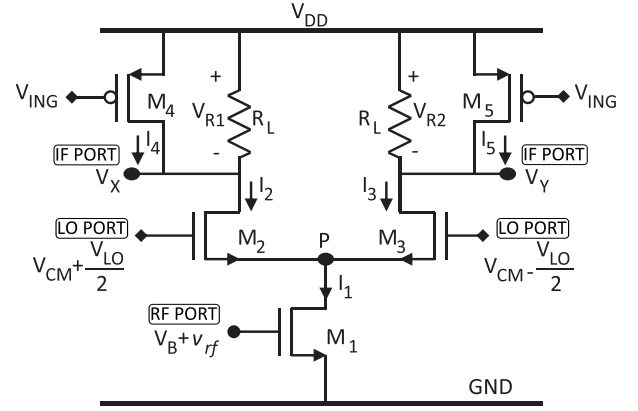


Fig. 2. Schematic of the static current injection mixer with pMOS current sources.

before the other one turns OFF. This degrades the mixer's linearity in the output. Providing a part of the switching stage's current, through external current sources, keeps V_X and V_Y higher than the limit determined in (1). Consequently, the mixer avoids signal compression in the output and achieves higher linearity with higher R_L and conversion gain than R_{L0} and CG_0 , respectively.

A. Static Current Injection Method

Considering a constant injection current of $I_{inj} = m_s I_1$, the current through R_L decreases to $(1 - m_s)I_1$ when either M_2 or M_3 is turned OFF. m_s is the static current injection ratio. The maximum load resistor, $R_{L-static}$ and the maximum conversion gain, CG_{static} , in this case, are

$$R_{L-static} = R_L|_{I_{inj}=m_s I_1} = \frac{1}{1 - m_s} R_{L0} \quad (5)$$

$$CG_{static} = \frac{1}{1 - m_s} \frac{2}{\pi} \frac{V_{R,max}}{V_{ov1}} = \frac{1}{1 - m_s} CG_0. \quad (6)$$

Although the maximum voltage drop across R_L is equal to (2), at LO zero-crossing points, the current splits equally between M_2 and M_3 . This causes V_{R1} and V_{R2} to drop as well. Therefore, at LO zero crossings

$$V_{R1} = V_{R2} = R_{L-static} \left(\frac{I_1}{2} - m_s I_1 \right). \quad (7)$$

Static injection current sources can be implemented as shown in Fig. 2 and with a pair of pMOS devices, M_4 and M_5 . The overdrive voltage of M_4 and M_5 , V_{ovinj} , is fixed by their gates bias voltage, V_{ING} . To maintain M_4 and M_5 in saturation at LO zero crossings, V_{R1} and V_{R2} should remain higher than V_{ovinj} . Therefore, using (7), the maximum current injection ratio, m_{s-max} , is determined by

$$m_{s-max} = \frac{\frac{V_{R,max}}{2} - V_{ovinj}}{V_{R,max} - V_{ovinj}}. \quad (8)$$

m_{s-max} is always less than 0.5 in (8) and reaches its maximum for very low V_{ovinj} . Therefore, in static current injection method, the signal compression at the output can be overcome for a limited improvement in conversion gain.

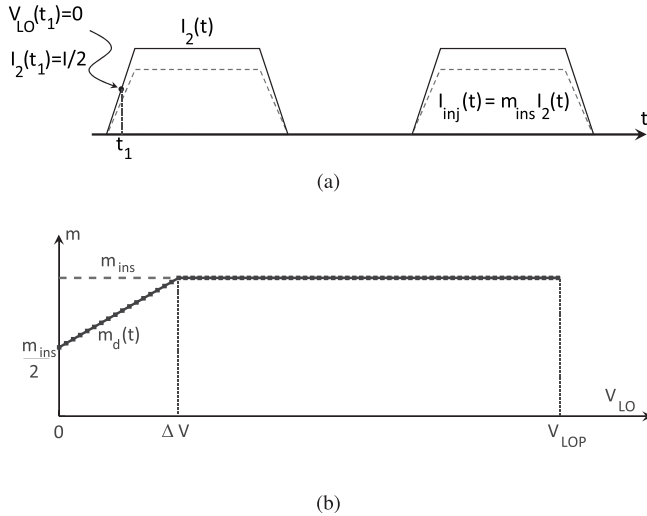


Fig. 3. (a) I_2 and the dynamically injected current into the drain of M_2 and (b) m_{ins} and $m(t)$ versus instantaneous LO amplitude.

Based on (6), signal compression due to only 5.2 dB of gain improvement with $V_{ovinj} = 0.05$ V and $V_{R_{max}} = 0.65$ V can be achieved.

B. Dynamic Current Injection Method

Fig. 3(a) shows the dynamic current injection concept in one branch of the mixer. I_{inj} and I_2 are represented by the dashed and solid lines, respectively. In positive half cycle of the LO signal, the injection current is a fraction of the current through M_2

$$I_{inj}(t) = m_{ins} I_2(t). \quad (9)$$

Equation (9) shows the injection current at each instant is a constant fraction of the instantaneous current through the switches instead of the overall mixer's current, I_1 . I_{inj} is $(1/2)m_{ins}I_1$ at LO zero crossings and reaches its maximum of $m_{ins}I_1$ determined by (9) in each period of the LO signal and when M_3 turns OFF. For dynamic current injection, the load resistor, $R_{L-dynamic}$, and the conversion gain, $CG_{dynamic}$, are determined by

$$R_{L-dynamic} = R_L |_{I_{inj}(t)=m_{ins}I_2(t)} = \frac{1}{1-m_{ins}} R_{L0} \quad (10)$$

$$CG_{dynamic} = \frac{1}{1-m_{ins}} CG_0. \quad (11)$$

In comparison to the static current injection, the first immediate advantage of this method is the elimination of voltage drop across the load resistor at the zero-crossing instances of the LO signal

$$V_R(t) = (1-m_{ins}) I_2(t) R_{L-dynamic} = I_2(t) R_{L0}. \quad (12)$$

As shown in (12), $V_R(t)$ for the dynamic current injection of Fig. 3 is independent of m_{ins} and equal to $V_R(t)$ for the simple mixer with R_{L0} as the load resistance. Therefore, increasing m_{ins} higher than 0.5, which is the asymptotic limit for the static current injection method becomes possible. Increasing m_{ins} increases the voltage conversion gain while based on (12), the

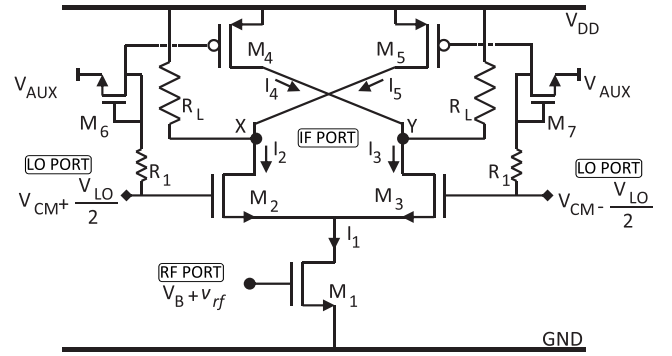


Fig. 4. Schematic of the dynamic current injection mixer (single-balanced implementation).

output voltages remain intact. This leads to the independence of the mixer's gain and linearity performance in ideal dynamic current injection. Unlike the static current injection ratio which is constant in the whole LO signal's period, the dynamic current injection ratio, $m_d(t)$, given by

$$m_d(t) = \frac{I_{inj}(t)}{I_1} = m_{ins} \frac{I_2(t)}{I_1} \quad (13)$$

is periodic. Assuming piecewise linear devices, m_{ins} and $m_d(t)$ are both shown in Fig. 3(b) versus a half period of the LO signal. V_{LOP} is the maximum amplitude of the LO signal, and ΔV is the minimum LO voltage imbalance required to turn OFF M_3 and steer the current completely to M_2 . As mentioned in Section II, ΔV is equal to $\sqrt{2}V_{ov2,3}$ where the channel-length modulation is neglected. Since

$$I_1 = I_2(t) + I_3(t) \quad (14)$$

$m_d(t)$ is $(1/2)m_{ins}$ at LO zero crossings and increases to m_{ins} when M_3 turns OFF. By changing M_2 to M_3 and replacing I_2 with I_3 , (9)–(13) remain the same for the other half period of the LO signal.

To implement dynamic current injection, a pMOS cross-coupled pair as shown in Fig. 4, has been used. At zero-crossing instances, the overdrive voltages of M_4 and M_5 are equal, and provide M_2 and M_3 with equal injection currents. In the positive half period of the LO signal, M_3 starts to turn OFF, and I_2 increases until all of I_1 passes through M_2 . While I_2 is rising in the positive half period of the LO signal, the overdrive voltage of M_5 , connected to $-(V_{LO}/2)$, also increases and its current reaches $m_{ins}I_1$ when M_3 turns OFF and $I_2 = I_1$. This procedure repeats for M_3 and M_4 in the next half period of the LO signal.

III. IMPLEMENTATION OF DYNAMIC CURRENT INJECTION IN SINGLE-BALANCED MIXER

A. Design Procedure

When $I_{inj} = 0$, (1)–(4) determine the maximum available gain without compromising the mixer's linearity. The instantaneous current injection ratio, required to achieve a higher conversion gain of $CG_{dynamic}$, can be found using (11),

and is

$$m_{\text{ins}} = 1 - \frac{CG_0}{CG_{\text{dynamic}}}. \quad (15)$$

Using (3) and (10), $R_{L\text{-dynamic}}$ necessary to deliver CG_{dynamic} is determined. To determine the size of the cross-coupled pair, the current injection is investigated at $|V_{\text{LO}}(t)| = \Delta V$, when either M_2 or M_3 turns OFF. Considering a piecewise linear current, the current injection reaches $m_{\text{ins}}I_1$, using (9), to maintain V_X and V_Y equal to $V_{X,Y_{\text{min}}}$ when the other branch of the mixer is turned OFF. Therefore, at $V_{\text{LO}}(t) = \Delta V$

$$I_2 = \frac{\mu_n C_{ox}}{2 \left(1 + \frac{(1 + \frac{\sqrt{2}}{2}) V_{ov2}}{E_c L_2}\right)} \left(\frac{W}{L}\right)_2 \left(1 + \frac{\sqrt{2}}{2}\right)^2 V_{ov2}^2 \quad (16)$$

$$I_5 = \frac{\mu_p C_{ox}}{2 \left(1 + \frac{V_{ov5} + \frac{\sqrt{2}}{2} V_{ov2}}{E_c L_5}\right)} \left(\frac{W}{L}\right)_5 \left(V_{ov5} + \frac{\sqrt{2}}{2} V_{ov2}\right)^2 \quad (17)$$

where in (16) and (17), E_c is the critical electrical field while μ_n and μ_p are the electron and hole mobilities, respectively. Using (16) and (17) and since $I_5(t) = m_{\text{ins}}I_2(t)$, the aspect ratio of M_5 is given by

$$\begin{aligned} \left(\frac{W}{L}\right)_5 &= m_{\text{ins}} \frac{\mu_n}{\mu_p} \left(\frac{(1 + \frac{\sqrt{2}}{2}) V_{ov2}}{V_{ov5} + \frac{\sqrt{2}}{2} V_{ov2}}\right)^2 \\ &\times \frac{1 + \frac{V_{ov5} + \frac{\sqrt{2}}{2} V_{ov2}}{E_c L_5}}{1 + \frac{(1 + \frac{\sqrt{2}}{2}) V_{ov2}}{E_c L_2}} \left(\frac{W}{L}\right)_2. \end{aligned} \quad (18)$$

Since I_2 is half of the current in (16), m_{ins} at the LO zero crossings is

$$\begin{aligned} m_{\text{ins}}|_{\text{zero crossings}} &= 2 m_{\text{ins}} \left(\frac{V_{ov5}}{V_{ov5} + \frac{\sqrt{2}}{2} V_{ov2}}\right)^2 \\ &\times \frac{1 + \frac{V_{ov5} + \frac{\sqrt{2}}{2} V_{ov2}}{E_c L_5}}{1 + \frac{V_{ov5}}{E_c L_5}}. \end{aligned} \quad (19)$$

As stated in Section II-B and shown in Fig. 3(b), m_{ins} is ideally constant in the whole period of the LO signal while the injection currents through M_5 and M_4 are varying periodically. Consequently, V_{ov5} is determined from (19) and is equal to

$$V_{ov5} = \left(1 + \frac{\sqrt{2}}{2}\right) V_{ov2} \times \frac{1}{1 + \frac{V_{ov5}}{E_c L_5}}. \quad (20)$$

The last term in (20) demonstrates short channel effect of dynamic current injection pMOS pair. Assuming L_5 is chosen large enough, (20) can be simplified to

$$V_{ov5} = \left(1 + \frac{\sqrt{2}}{2}\right) V_{ov2}. \quad (21)$$

As shown in Fig. 5, in $2\Delta T$ of each period of the LO signal, M_2 and M_3 are ON simultaneously. The noise contribution of both M_4 and M_5 appears in the output. When the mixer

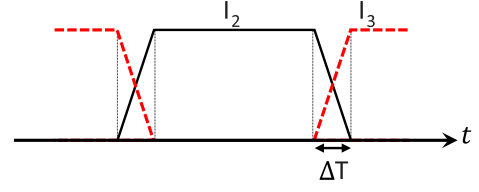


Fig. 5. Current commutation between M_2 and M_3 during time.

current is steered to M_2 or M_3 , one of M_4 and M_5 turns OFF and only half of the cross-coupled pair produces noise in $T_{\text{LO}} - 2\Delta T$, where T_{LO} is the LO signal period. The output noise contribution of the pMOS cross-coupled pair, $\hat{V}_{o,n}^2$ is given by

$$\hat{V}_{o,n}^2 = \left(1 + \frac{2\Delta T}{T_{\text{LO}}}\right) (g_{m5} R_L)^2 \hat{V}_{n,5}^2. \quad (22)$$

In deriving (22), $\hat{V}_{n,5}^2$ and g_{m5} are assumed to be equal to $\hat{V}_{n,4}^2$ and g_{m4} , respectively. Because the cross-coupled pair is placed in the output stage, (22) holds for both high-frequency and low-frequency (flicker) noise contribution. Noise behavior of the rest of the current commutating mixer is analyzed in [14] and is not included here.

The high-frequency input referred noise of the cross-coupled pair after simplification is

$$\hat{V}_{in,n}^2 = \left(\frac{T_{\text{LO}} + 2\Delta T}{T_{\text{LO}} - 2\Delta T}\right) \left(\frac{\pi^2 \gamma kT}{g_{m1}}\right) \frac{g_{m5}}{g_{m1}}. \quad (23)$$

The second term in (23) is the noise contribution of the transconductance stage of the mixer. If g_{m5} is significantly lower than g_{m1} , the noise contribution of the cross-coupled pair is negligible compared with the input referred noise due to the transconductance stage.

The effect of the cross-coupled pair on flicker noise can be minimized by increasing the size of M_4 and M_5 . Although the equivalent parasitic capacitance of the pair is more significant due to larger pMOS devices, it is acting as the output IF filter of the mixer and does not affect gain, linearity, or RF bandwidth.

B. Design Example

The mixer is designed for 0.13- μm CMOS technology node. The overdrive voltage of the transconductance and switching stages is 0.3 and 0.1 V, respectively, to guarantee high linearity and fast switching in the mixer. The current is limited to 2 mA from a 1.2 V supply voltage. $V_{X,Y_{\text{min}}}$, determined by (1) is, therefore, 0.5 V. An additional margin of 0.2 V is added to the minimum output voltage to ensure no linearity degradation in the output ($V_{X,Y_{\text{min}}} = 0.7\text{V}$). Using the design procedure in Section III-A and using (3) and (4), R_{L0} and CG_0 are 250 Ω and 0.5 dB, respectively. Therefore, to design a dynamic current injected mixer with 12.5 dB of conversion gain, $m_{\text{ins}} = 0.75$ is required, using (11). Also, $R_{L\text{-dynamic}}$ is 1 $k\Omega$, determined by (10).

The overdrive voltage of the cross-coupled pair is found to be 0.15 V using (21) and (20) while $(W/L)_5 = 1.19(W/L)_2$,

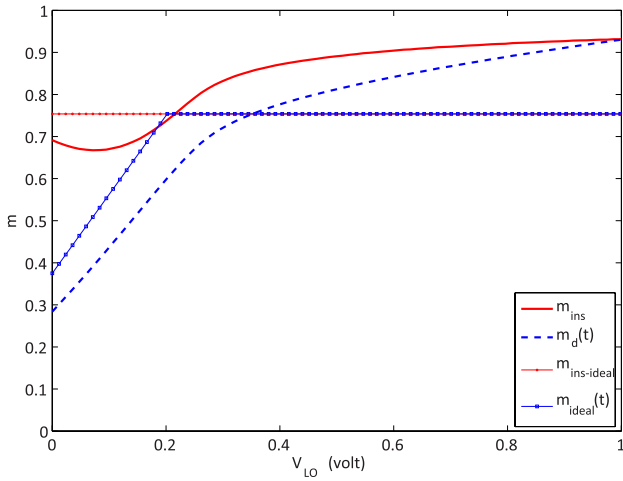


Fig. 6. m_{ins} and $m_d(t)$ of the pMOS cross-coupled pair along with the ideal case of $m_{ins} = 0.75$.

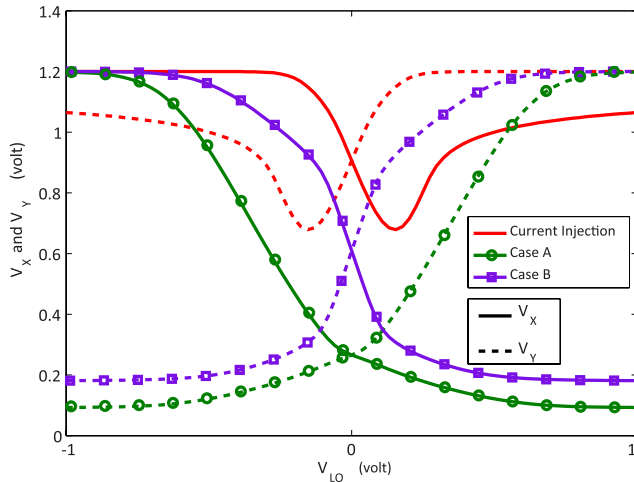


Fig. 7. Output voltages of all three SBMs versus $V_{LO_{ins}}$.

determined using (18). In the calculation of the aspect ratio of the pMOS cross-coupled devices, using (18), (μ_n/μ_p) is estimated by low-field mobilities in $0.13\text{-}\mu\text{m}$ CMOS technology and is 4.6. Also, E_c is 1.5×10^6 V/m.

The designed SBM is simulated and optimized using Spectre in Cadence and Global Foundries (formerly IBM) design kit, CMOS8RF, for $0.13\text{-}\mu\text{m}$ CMOS technology. To investigate the dynamic current injection method by itself, the transconductance stage is kept to its most basic implementation, shown in Fig. 1 and when $I_{inj} = 0$. The simulations have been carried out for current commuting mixers with the same power consumptions, device aspect ratios and sizes in three cases.

Case A: Simple current commuting mixer with same R_L as the dynamic current injection mixer.

Case B: Simple current commuting mixer with R_L optimized for maximum conversion gain.

Case C: The dynamic current injection mixer.

Case A is essentially the proposed mixer without its dynamic current injection mechanism. Comparing the same

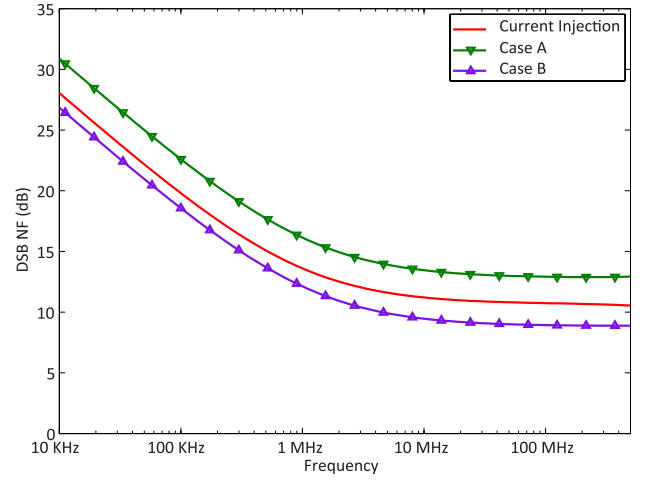


Fig. 8. Simulated DSB NF of the designed mixers versus IF frequency.

TABLE I
PART SIZES OF THE MIXER FOR THREE CASES

Part	$(\frac{W}{L})_1$	$(\frac{W}{L})_{2,3}$	$(\frac{W}{L})_{4,5}$	$R_{L_{dy}}$	R_{L_A}	R_{L_B}
Value	$\frac{17}{0.12}$	$\frac{55}{0.12}$	$\frac{350}{1}$	1k	1k	0.6k

mixer with and without dynamic current injection will demonstrate the improvements in IIP3, P_{1dB} , voltage conversion gain, and NF reached by the proposed method. Case B is also studied here to investigate the improvements in IIP3 and P_{1dB} when the simple mixer provides the same gain as the proposed mixer. Because the simple mixer fails to deliver the same gain, it is optimized to deliver maximum voltage conversion gain.

The values used in the simulations are given in Table I where $R_{L_{dy}}$, R_{L_A} , and R_{L_B} are the load resistors for dynamic current injection mixer, Case A, and Case B, respectively. All mixers consume 2 mA current from a 1.2 V supply voltage. To bias the switching devices and the cross-coupled pair together, $V_{ov5} = 0.2$ V is used in the simulations and $(W/L)_5 = 0.83(W/L)_2 = (380/1 \mu\text{m})$ is determined, using (18). Short channel effect on μ_n and μ_p is neglected and (18) overestimates the cross-coupled pair's aspect ratio. Therefore, the size of the cross-coupled pair has been tuned in simulations for more accurate current injection and is $(350/1 \mu\text{m})$.

Fig. 6 shows m_{ins} and $m_d(t)$ versus instantaneous LO voltage in a half period. For small V_{LO} amplitudes, the current injection ratio is lower than the ideal case studied in Section II-B. Smaller $m_d(t)$ results in $V_{X,Y}(t) < V_{X,Y-ideal}(t)$, keeping the cross-coupled pair well into saturation region. $V_{X,Y-ideal}(t)$ denotes output voltages, V_X and V_Y in the ideal dynamic current injection case. As the LO amplitude increases, $m_d(t)$ also increases beyond its designed value.

The variation of the output voltages at each instance of the LO signal is shown in Fig. 7. V_X and V_Y reach their minimum when the other switch turns OFF. The output voltages start to increase again due to the extra current injection to the output nodes at larger LO signal amplitudes. For Cases A and B, output voltages are dropping far lower than the minimum

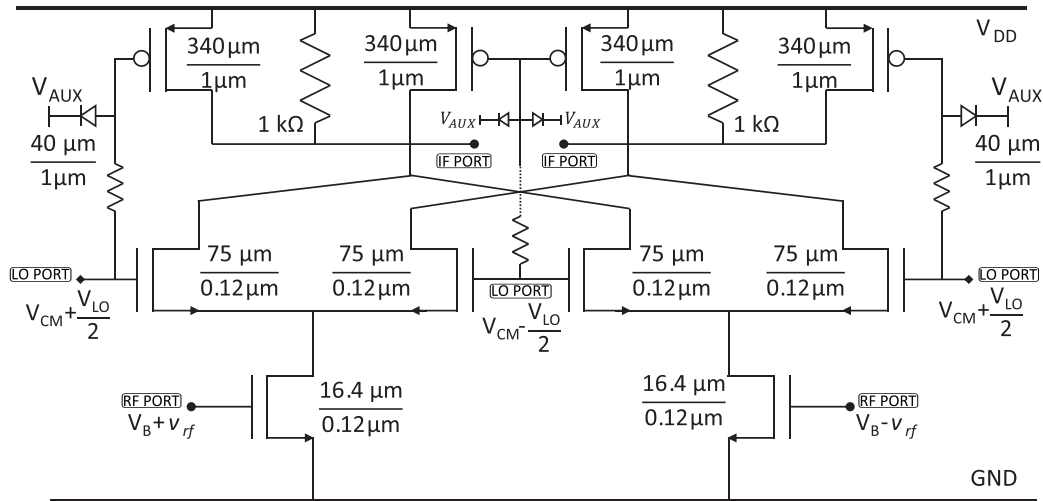


Fig. 9. Schematic of the proposed DBM mixer.

TABLE II
COMPARISON OF DYNAMIC CURRENT INJECTION MIXER
AND CONVENTIONAL MIXERS ($P_{LO} = 4$ dBm)

	units	Case A	Case B	Dynamic Current Injection Mixer
Conversion Gain	dB	-1.8	9.4	12
Input P_{1dB}	dBm	4.8	-9.26	-5.2
IIP3	dBm	-1.7	0	6.25
DSB NF (200 MHz)	dB	12.5	8.5	10.25
DSB NF (20 KHz)	dB	28.2	24.15	25

output voltage limit, estimated by (1). However, this limit is maintained for the proposed mixer. Therefore, compared with dynamically current injected mixer degraded linearity is expected for both Cases A and B.

Table II summarizes the simulation results of the mixers in these three cases. In Case A, V_X and V_Y reduce dramatically below $V_{X,Y,min}$, determined to maintain the proper operation of the mixer. This results in a negative conversion gain of -1.8 dB. Although the conversion gain of the mixer can be improved by optimizing the load resistance of the mixer and reaches 9.4 dB for Case B, it is still lower than the 12 dB gain achieved in the dynamically current injected mixer.

The proposed method also results in a more linear mixer with 6.25-dBm IIP3 compared with -1.7 and 0 dBm for Cases A and B, respectively. Fig. 8 shows the DSB NF of the simulated mixers. Due to the low conversion gain in Case A, its high-frequency NF is 12.5 dB. The NF of the proposed mixer is 10.25 dB. This is only 1.75 dB higher than the NF of Case B.

The double-balanced version of the proposed mixer is shown in Fig. 9, and it is the circuit that was fabricated and whose results are presented in Section IV.

IV. DOUBLE-BALANCED MIXER IMPLEMENTATION AND MEASUREMENT RESULTS

To validate the dynamic current injection method, a double-balanced mixer with the dynamic current injection

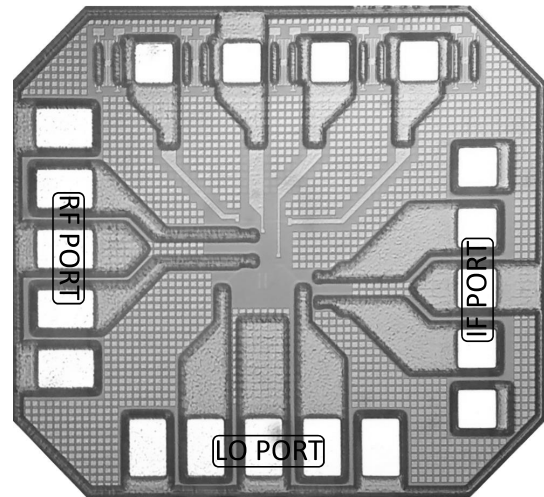
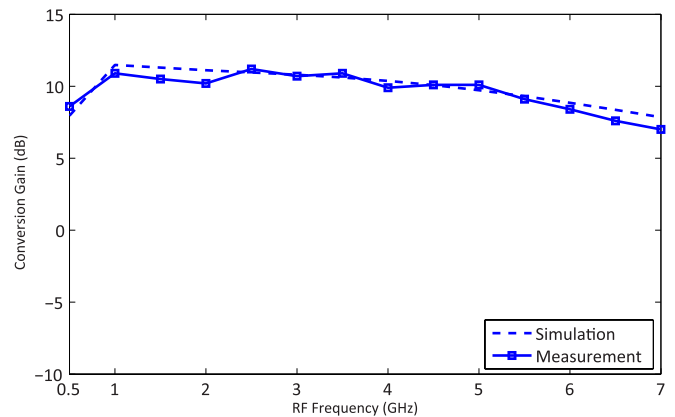


Fig. 10. Microphotograph of the fabricated DBM.


 Fig. 11. Measured and simulated conversion gain versus RF frequency. $F_{IF} = 200$ MHz, $F_{LO} = F_{RF} + F_{IF}$, and $P_{LO} = 4$ dBm.

and $m_{ins} = 0.75$ is designed and fabricated using IBM 0.13- μ m RF CMOS. The components values are shown in Fig. 9. The overdrive voltages of the devices are the same

TABLE III
PERFORMANCE SUMMARY AND COMPARISON TABLE

	units	This Work	[1]	[2]**	[3]	[4]	[5]	[7]	[9]	[10]
RF Frequency	GHz	0.5–6.5	0.3–1.2	2.1	2–10	1–5.5	0.77	1	5.2	1–10
IF bandwidth	GHz	0.3	–	–	–	–	–	–	–	0.1–1
LO power	dBm	4	–	6	–	0	-5	–	-5	0
Conversion gain	dB	10	8.8	15	24–9	17.5	17	7	12	3–8
Input P_{1dB}	dBm	-2.4	-13.2– -8.8	–	-4– -19	-10.5	–	-15	-7	-16– -12.2
IIP3	dBm	9.52	-4.2– -0.8	15	3.5– -12	0.84	-4.9	–	4	-7– -4
DSB NF	dB	13	<4.8	14	8–23	3.9	7.9	14	10.6	8.3–12
RF-IF isolation	dB	64	–	–	–	–	–	–	55	–
LO-IF isolation	dB	59.76	–	–	–	–	–	–	54	>40
DC power	mW	4.5	24	8	2.4–18	34.5	5.6	14.4	4.6	8.4
Chip area	mm ²	0.015•	0.56•	–	0.19•	0.315•	0.89	0.72	0.545	0.28•
FOM	dB	15.22	10.39	16.96	10.44	14.89	15.66	–	15.77	9.45

* Measured results taken at 2 GHz.

** Simulation results.

• Core area.

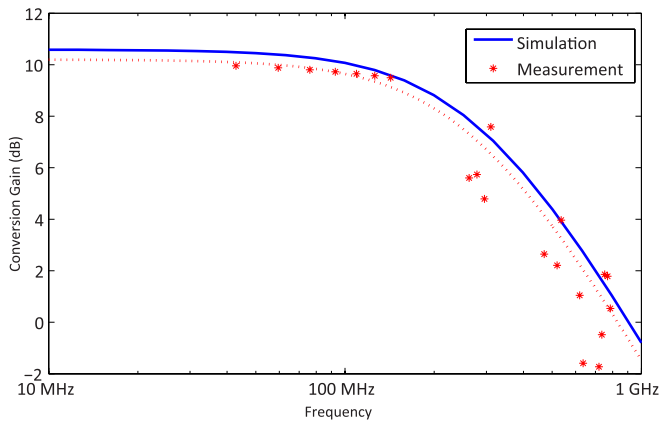


Fig. 12. Measured and simulated conversion gain versus IF frequency. $F_{RF} = 2$ GHz and $P_{LO} = 4$ dBm.

as the single-balanced design. A microphotograph of the fabricated chip is shown in Fig. 10. The chip core occupies an area of 0.015 mm², excluding the bonding pads. The circuit consumes 4.5 mW of dc power from a 1.2 V supply.

In DBM implementation, there are two dynamic current injection connected to each output nodes. In each half cycle of the LO signal, one of the current injection devices provides the required injection current to the switching stage.

Two external passive baluns are used to generate the differential RF and LO signals. An external differential to single ended buffer is used to measure the mixer's performance with spectrum analyzer. Fig. 11 shows the measured and simulated conversion gain of the mixer from 0.5 to 7 GHz. The dynamic current injection mixer shows a 3-dB gain bandwidth from 0.5 to 6.5 GHz. This large bandwidth was expected due to inductor-less design and limiting the modifications to the IF stage of the mixer.

Fig. 12 shows the measured and simulated results of conversion gain versus IF frequency. IF bandwidth of 300 MHz is achieved in the proposed mixer. As mentioned in Section III-B, the large pMOS cross-coupled pair acts as the IF filter

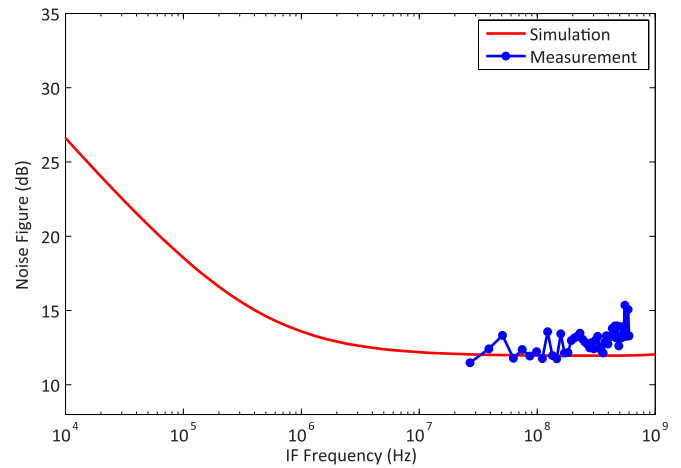


Fig. 13. Measured and simulated DSB NF versus IF frequency. $F_{RF} = 2$ GHz, $F_{LO} = F_{RF} + F_{IF}$, and $P_{LO} = 4$ dBm.

and limits the IF bandwidth. The measurement results provided for the conversion gain of the mixer agree with the simulation results, with 0.5-dB degradation at 2 GHz, giving 10.2 dB. Also, the conversion gain's maximum is 11.2 dB at 2.5 GHz.

Measured and simulated NF are shown in Fig. 13 for $f_{LO} = 2$ GHz. At IF frequency of 200 MHz, NF is 13 dB while the simulation result shows 12.34 dB. The measured results are provided for frequencies higher than 10 MHz due to the calibration limitation of the measurement instruments. Measured and simulated P_{1dB} are -2.4 and -3.4 dBm, respectively, at $f_{RF} = 2$ GHz and $P_{LO} = 4$ dBm. Measurement results for the IIP3 of the mixer is shown in Fig. 14. The measured IIP3 and simulated IIP3 at this frequency are 9.52 and 10.56 dBm, respectively. Isolation of the IF to RF and LO signals is also better than 59 dB in whole frequency band. A summary of the measured results and a comparison with other works are provided in Table III.

To have a fair comparison, a figure of merit (FOM) is also

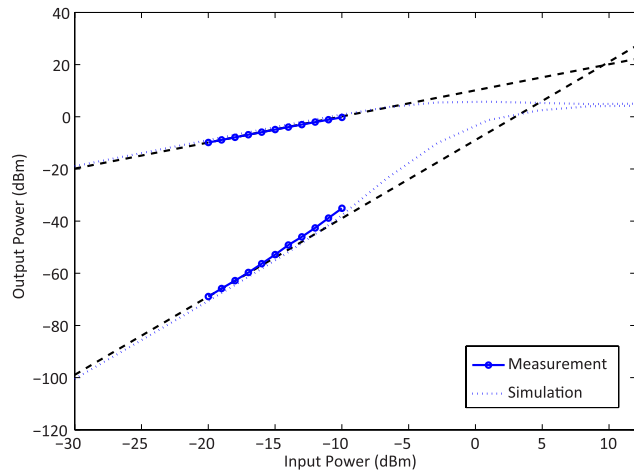


Fig. 14. Measured and simulated IIP3. $F_{RF} = 2$ GHz, $F_{IF} = 200$ MHz, $F_{LO} = F_{RF} + F_{IF}$, and $P_{LO} = 4$ dBm.

included in Table III [12]

$$\text{FOM} = 10 \log \left(\frac{10^{\frac{G}{20}} \cdot 10^{\left(\frac{IIP3-10}{20}\right)}}{10^{\frac{NF}{10}} \cdot P} \right). \quad (24)$$

In (24), the FOM reflects four of the most important metrics in any mixer: IIP3, NF, voltage conversion gain, G , and power consumption, P . Calculated FOM of the proposed mixer is 15.2 dB and is comparative to other mixers. Please note the size of the mixer is considerably lower than the previously reported designs.

V. CONCLUSION

A highly linear mixer with boosted gain, based on conventional Gilbert cell is demonstrated in this paper. The use of cross-coupled pair to inject dynamic current into the IF stage is the mechanism used to maintain a high linearity while improving the gain. Experimental test on fabricated prototype showed 10 dB conversion gain alongside 9.5-dBm IIP3.

ACKNOWLEDGMENT

The authors would like to thank CMC Microsystems, Kingston, ON, Canada for chip fabrication arrangements.

REFERENCES

- [1] S. He and C. E. Saavedra, "Design of a low-voltage and low-distortion mixer through Volterra-series analysis," *IEEE Trans. Microw. Theory Techn.*, vol. 61, no. 1, pp. 177–184, Jan. 2013.
- [2] M. Mollaipour and H. Miar-Naimi, "An improved high linearity active CMOS mixer: Design and Volterra series analysis," *IEEE Trans. Circuits Syst. I, Reg. Papers*, vol. 60, no. 8, pp. 2092–2103, Aug. 2013.
- [3] M. Wang and C. E. Saavedra, "Reconfigurable broadband mixer with variable conversion gain," in *IEEE MTT-S Int. Microw. Symp. Dig.*, Jun. 2011, pp. 1–4.
- [4] S. S. K. Ho and C. E. Saavedra, "A CMOS broadband low-noise mixer with noise cancellation," *IEEE Trans. Microw. Theory Techn.*, vol. 58, no. 5, pp. 1126–1132, Mar. 2010.

- [5] D.-Y. Yoon, S.-J. Yun, J. Cartwright, S.-K. Han, and S.-G. Lee, "A high gain low noise mixer with cross-coupled bleeding," *IEEE Microw. Wireless Compon. Lett.*, vol. 21, no. 10, pp. 568–570, Oct. 2011.
- [6] H. Darabi and J. Chiu, "A noise cancellation technique in active RF-CMOS mixers," *IEEE J. Solid-State Circuits*, vol. 40, no. 12, pp. 2628–2632, Dec. 2005.
- [7] H.-J. Wei, C. Meng, H.-I. Chien, H.-L. Lu, J.-S. Syu, and G.-W. Huang, "Flicker noise and power performance of CMOS Gilbert Mixers using static and dynamic current-injection techniques," in *Proc. Asia-Pacific Microw. Conf.*, 2010, pp. 542–545.
- [8] D. Cordova, S. Bampi, and E. Fabris, "A CMOS down-conversion mixer with high IIP2 and IIP3 for multi-band and multiple standards," in *Proc. 27th Symp. Integr. Circuits Syst. Design (SBCCI)*, Sep. 2014, pp. 1–7.
- [9] H.-K. Chiou, K.-C. Lin, W.-H. Chen, and Y.-Z. Juang, "A 1-V 5-GHz self-bias folded-switch mixer in 90-nm CMOS for WLAN receiver," *IEEE Trans. Circuits Syst. I, Reg. Papers*, vol. 59, no. 6, pp. 1215–1227, Jun. 2012.
- [10] H. Zijie and K. Mouthaan, "A 1-to 10-GHz RF and wideband IF cross-coupled Gilbert mixer in 0.13- μ m CMOS," *IEEE Trans. Circuits Syst. II, Exp. Briefs*, vol. 60, no. 11, pp. 726–730, Nov. 2013.
- [11] J.-B. Seo, J.-H. Kim, H. Sun, and T.-Y. Yun, "A low-power and high-gain mixer for UWB systems," *IEEE Microw. Wireless Compon. Lett.*, vol. 18, no. 12, pp. 803–805, Dec. 2008.
- [12] V. Vidojkovic, J. van der Tang, A. Leeuwenburgh, and A. H. M. van Roermund, "A low-voltage folded-switching mixer in 0.18- μ m CMOS," *IEEE J. Solid-State Circuits*, vol. 40, no. 6, pp. 1259–1264, Jun. 2005.
- [13] M.-M. Mohsenpour and C. E. Saavedra, "Method to improve the linearity of active commutating mixers using dynamic current injection," in *IEEE MTT-S Int. Microw. Symp. Dig.*, May 2016, pp. 1–4.
- [14] H. Darabi and A. A. Abidi, "Noise in RF-CMOS mixers: A simple physical model," *IEEE J. Solid-State Circuits*, vol. 35, no. 1, pp. 15–25, Jan. 2000.



Mohammad-Mahdi Mohsenpour (M'14) received the B.Sc. degree in electrical engineering from the University of Mazandaran, Babolsar, Iran, in 2009, and the M.Sc. degree in communications engineering-fields and waves from the University of Tehran, Tehran, Iran, in 2012. He is currently pursuing the Ph.D. degree with the Gigahertz Integrated Circuits Group, Queen's University, Kingston, ON, Canada.



Carlos E. Saavedra (S'92–M'98–SM'05) received the B.Sc. degree in electrical engineering from the University of Virginia, Charlottesville, VA, USA, in 1993, and the Ph.D. degree in electrical engineering from Cornell University, Ithaca, NY, USA, in 1998.

From 1998 to 2000, he was a Senior Engineer with Millitech Corporation. In 2000, he joined Queen's University, Kingston, ON, Canada, where he is currently a Professor. He served as the Graduate Chair of the Department of Electrical and Computer Engineering (ECE) from 2007 to 2010.

Dr. Saavedra was a member of the IEEE RFIC Symposium from 2008 to 2011. He is a member of the TPRC of the IEEE International Microwave Symposium (IMS) and the IEEE NEWCAS Conference Steering Committee. He was a three-time recipient of the third-year ECE undergraduate teaching award at Queen's University. He is the former Section Chair of the Natural Sciences and Engineering Research Council of Canada Discovery Grants Evaluation Group 1510 and the former Chair of the IEEE MTT-S Technical Coordinating Committee 22 on Signal Generation and Frequency Conversion. He served on the Steering and Technical Program Committees of the 2012 IEEE IMS. He is an associate editor of the IEEE TRANSACTIONS ON MICROWAVE THEORY AND TECHNIQUES.